T−g and Rheological Properties of Triazine-Based Molecular Glasses: Incriminating Evidence Against Hydrogen Bonds

ARTICLE *in* THE JOURNAL OF PHYSICAL CHEMISTRY B · NOVEMBER 2009

Impact Factor: 3.3 · DOI: 10.1021/jp905268a · Source: PubMed

6 AUTHORS, INCLUDING:

Danny Pagé
Royal Military College of Canada
23 PUBLICATIONS **154** CITATIONS

SEE PROFILE

Olivier Lebel
Royal Military College of Canada
24 PUBLICATIONS **390** CITATIONS

SEE PROFILE

T_g and Rheological Properties of Triazine-Based Molecular Glasses: Incriminating Evidence Against Hydrogen Bonds

André Plante,[†] Damien Mauran,[‡] Simão P. Carvalho,[†] J. Y. S. Danny Pagé,[†] Christian Pellerin,[‡] and Olivier Lebel*[,†]

Department of Chemistry and Chemical Engineering, Royal Military College of Canada, Kingston, Ontario, K7K 7B4 Canada, and Département de Chimie, Université de Montréal, Montréal, Québec, H3C 3J7 Canada

Received: June 4, 2009; Revised Manuscript Received: August 7, 2009

Bis(mexylamino)triazines have been identified as a family of compounds showing an exceptional propensity to form glassy phases as opposed to crystals. The particularities of this family of compounds are their ability to self-assemble through hydrogen bonding in well-defined patterns to form supramolecular aggregates which pack poorly and the wide range of glass transition temperatures (T_g) that can be attained through minor structural modifications. Representative bis(mexylamino)triazines were studied by rheology to establish correlations between their rheological properties and their molecular structure, and all compounds were found to behave in a similar fashion except for the temperature at which glass transition takes place. FTIR and NMR spectroscopy experiments were performed on the molecular glasses studied herein; comparisons between the viscosity, T_g, hydrogen bonding, and association constant (K_a) in $CDCl_3$ solution have revealed a relationship between the rheological properties, the T_g of the molecular glasses, and the extent and strength of hydrogen bonding present in the material.

Introduction

Several properties of polymers, including their thermal, mechanical, and rheological properties, depend not only on their molecular structures but also on several factors such as their molecular weight, polydispersity, and tacticity,[1] the presence of crystalline or microstructured domains,[2] and the thermomechanical history of the material including processing conditions, annealing, etc.[3] However, for their small-molecule counterparts, called molecular glasses or amorphous molecular materials,[4] the effect of several of these factors on the properties of the materials is greatly diminished. Variations in molecular weight are nonexistent (at least with pure samples) since molecular glasses are monodisperse species; partial crystallinity is highly undesirable as it usually results in rapid crystallization of the whole sample;[5] and while they show some degree of hysteresis,[6] the greater mobility of small molecules allows the materials to equilibrate toward the most stable amorphous form even at temperatures below their glass transition,[7] attenuating the effect of processing on properties. While this limits the range of properties that can be achieved with a single compound, it allows one to generate materials with the desired properties more reliably through strategic molecular design and synthesis.

While the effect of certain structural elements on glass transition temperature (T_g) has been established, the relationship between molecular structure and T_g is only marginally understood and only within certain classes of compounds.[4,8] Furthermore, there have been even fewer attempts to understand the effect of molecular structure on the mechanical or rheological properties of molecular glasses.[9]

Recently, we have begun to investigate 4,6-bis(mexylamino)-1,3,5-triazines as a family of molecular glasses in which most compounds synthesized so far readily form glassy phases and show an exceptional resistance to crystallization.[10] The particularity of this family of compounds lies in their ability to form supramolecular aggregates through hydrogen bonding along specific patterns.[10,11] As opposed to popular belief, compounds of this family were found to self-assemble through hydrogen bonds in the amorphous state, and a correlation was demonstrated between disruption of the hydrogen bonds and the physical changes observed as the compounds undergo glass transition.[11] Furthermore, a strikingly wide range of T_g were achieved only by changing the functionality of the "headgroup" at the 2-position of the triazine ring.[12] To further our knowledge of the relationship between molecular structure and physical properties in this class of compounds, representative compounds were selected to form two test sets: (1) compounds **1**−**9a** which consist of methyl-substituted derivatives with various functional groups, except for tertiary amine **6**, which was selected instead of the dimethylamino derivative because of the poor glass-

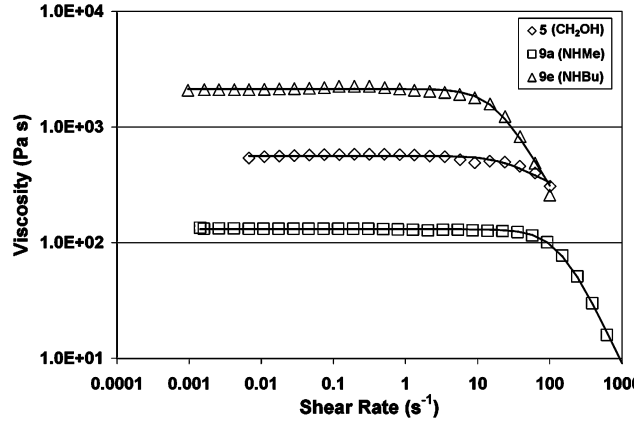

Figure 1. Flow curves of molecular glasses **5**, **9a**, and **9e** at T_g + 35 °C. Carreau regression is shown for each data set as a full line.

* Author to whom correspondence may be addressed. E-mail: olivier.lebel@rmc.ca.
[†] Royal Military College of Canada.
[‡] Université de Montréal.

10.1021/jp905268a CCC: $40.75
Published on Web 10/21/2009

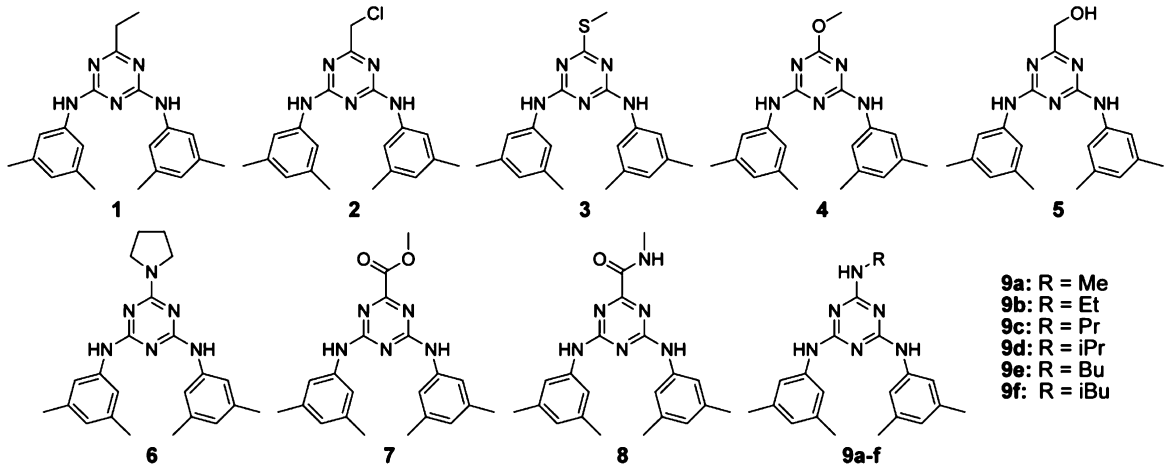

forming ability of the latter and (2) secondary amines **9a**−**f** with varying alkyl chain lengths ranging from methyl to butyl and including both linear and branched chains.

Herein, compounds **1**−**9** were studied by melt rheology to probe their behavior in the molten state to assess their properties relative to other types of amorphous materials and to monitor the effect of molecular association on their rheological properties. Glasses **1**−**9** were then studied by variable-temperature FTIR spectroscopy to attempt to establish relationships between their rheological properties and hydrogen bonding. Finally, the association constants (K_a) of compounds **1**−**9** in $CHCl_3$ solution were determined by variable-concentration ^1H NMR spectroscopy. For all molecular glasses studied herein, the relative fraction of N−H groups engaged in hydrogen bonding in the bulk material (subsequently referred to as hydrogen bonding index)[13] was found to impact the rheological properties of the materials. Not surprisingly, T_g was found to increase in a roughly linear fashion with association constant, though it is obvious that other structural elements impact T_g.

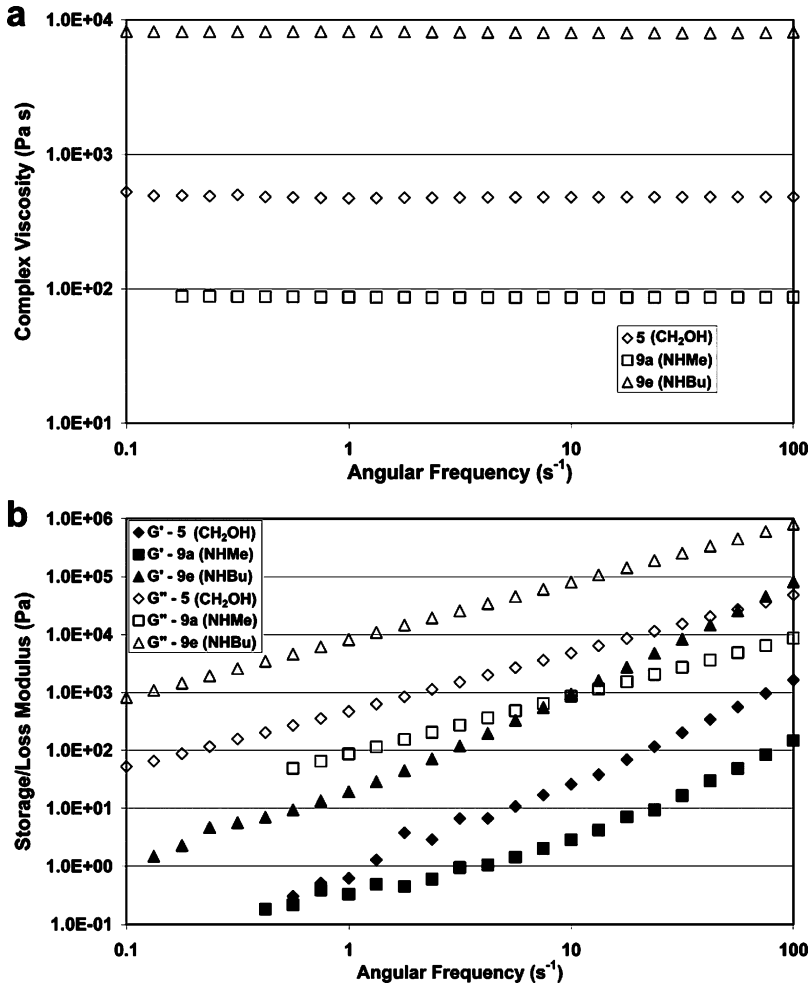

Figure 2. Angular frequency scans of compounds **5**, **9a**, and **9e** at T_g + 35 °C. (a) Complex viscosity. (b) Storage modulus (G') and loss modulus (G'').

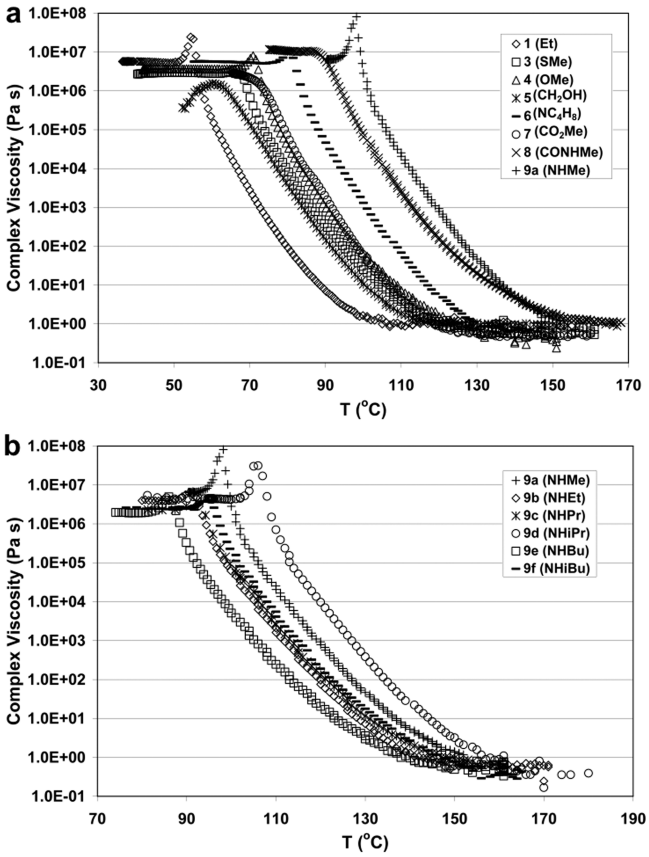

Figure 3. Complex viscosity as a function of temperature for (a) molecular glasses with various headgroups **1**−**9a** and (b) alkylamino-substituted glasses **9a**−**9f**. Only the heating scans are shown for clarity.

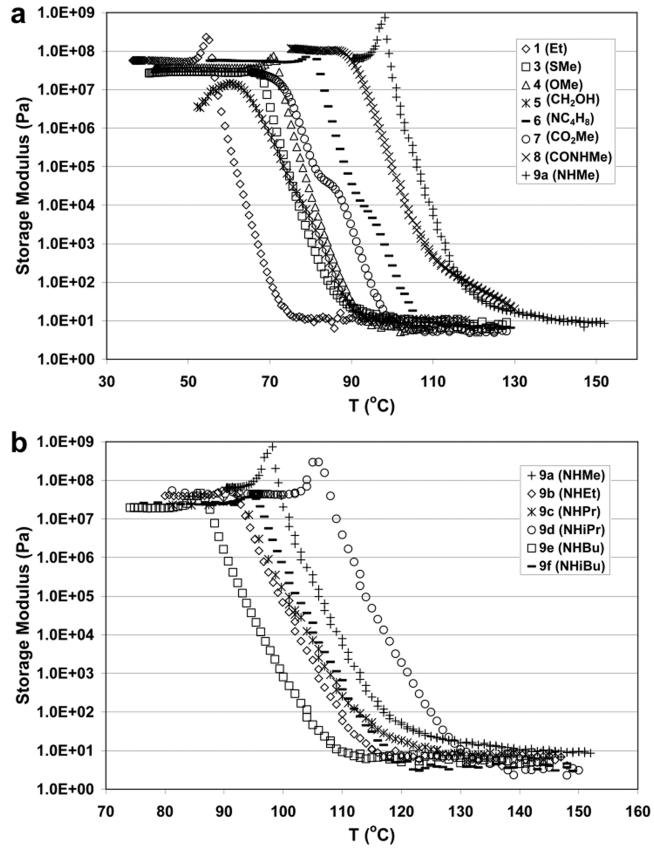

Figure 4. Storage modulus (G') as a function of temperature for triazine-based molecular glasses (a) **1**−**9a** and (b) **9a**−**9f**. For clarity purposes, only the heating scans are shown.

Experimental Section

Compounds **1**−**9** were prepared according to literature procedures.[10,12]

Molding of Discs of Compounds 1−9. Discs of compounds **1**−**9** were molded by bringing the compounds to 160 °C (for compounds **2**, **5**, **7**, and **8**) or 200 °C (for all other compounds) in a crucible and casting the molten compound in a circular brass mold with 25 mm diameter and 2 mm deep; the samples were then allowed to cool to room temperature at which point they delaminated and were removed from the mold.

Parallel-Plate Rheology of Compounds 1−9. General. Discs of compounds **1**−**9** were mounted at T_g + 100 °C on a Physica US200 parallel-plate rheometer equipped with plates 25 mm in diameter, and then the sample was kept at that temperature for 5 min to ensure complete melting before setting the gap between the two plates. The gap was then adjusted so that the sample occupied the entire space between the plates (typically between 1.2 and 1.5 mm). The temperature was then allowed to equilibrate at the set value for 15 min. All tests were performed under ambient atmosphere and were repeated at least in duplicate to ensure reproducibility of the data.

Flow Scans. The samples of compounds **5**, **9a**, and **9f** were scanned at T_g + 35 °C (94, 129, and 100 °C, respectively). The samples were then scanned in rotational mode at shear rates ranging from 0.001 to 100 s^{-1} (for compounds **5** and **9f**) or from 0.001 to 1000 s^{-1} (for compound **9a**) for a constant period of 10 s for each data point, and viscosity was recorded for each shear rate applied.

Angular Frequency Scans. The samples of compounds **5**, **9a**, and **9f** were scanned at T_g + 35 °C (94, 129, and 100 °C, respectively). The samples were scanned in oscillatory mode at a constant shear strain of 0.1% for 25 different angular frequencies ranging from 0.001 to 100 s^{-1}, and complex viscosity, storage modulus (G'), and loss modulus (G'') were recorded for each frequency.

Temperature Scans. The samples of compounds **1**−**9** were scanned in a cooling−heating cycle in oscillatory mode between roughly T_g + 60 to T_g + 80 °C and T_g − 20 to T_g − 10 °C at a rate of approximately 2 °C/min with a constant amplitude of 0.1% and a constant frequency of 10 s^{-1}. Complex viscosity, storage modulus (G'), and loss modulus (G'') were recorded in intervals of 30 s.

Variable-Temperature FTIR Spectroscopy. Temperature-controlled infrared spectra of compounds **1**−**9** were recorded from 30−40 °C to 160−200 °C, depending on their T_g, using a Tensor 27 FTIR spectrometer (Bruker Optics) equipped with a liquid nitrogen-cooled MCT detector. The samples were deposited on a preheated diamond crystal of a Golden Gate (Specac) single reflection attenuated total reflection (ATR) accessory to prevent crystallization. Spectra were recorded every 10 °C at a cooling/heating rate of 2 °C/min by averaging 50 scans with a 4 cm^{-1} resolution. In all cases, the background spectrum was obtained at the sample temperature since the IR transmission of diamond is strongly temperature-dependent. An extended ATR correction was applied to limit the effect of optical dispersion on the spectra.

Variable-Concentration ^{1}H NMR. Samples of known concentration were prepared by dissolving an appropriate amount of the desired compound in 1 mL of $CDCl_3$ which was previously filtered through a pad of basic aluminum oxide to remove traces of acid. The spectra were then recorded at 298 K using a Varian Mercury 300 or Bruker Avance 400

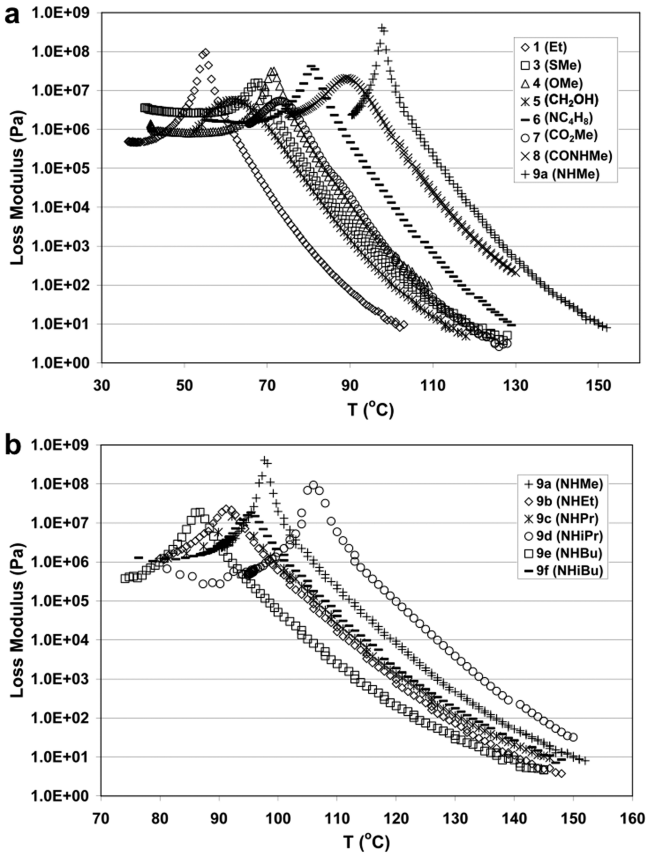

Figure 5. Loss modulus (G') as a function of temperature for triazine-based molecular glasses (a) **1**−**9a** and (b) **9a**−**9f**. For clarity purposes, only the heating scans are shown.

spectrometer on samples ranging from 1 mM to either 1 M or saturation in concentration, and the association constants were calculated by plotting the chemical shifts of the −NH groups as a function of concentration using the WinEQNMR2 software.[14]

Results and Discussion

Melt Rheology of Molecular Glasses 1−9. The dependence of viscosity on shear rate in the rotational mode was first established with representative compounds **5**, **9a**, and **9e** at T_g + 35 °C,[15] and the flow curves are shown in Figure 1. All three compounds were found to behave as Newtonian fluids at low shear rate and start displaying non-Newtonian behavior from 10 s^{-1} for compounds **5** and **9e** and from 50 s^{-1} for compound **9a** as evidenced by a sharp decrease in viscosity. The Carreau equation[16] was used to model the viscosity profiles for all three compounds, and the curves are displayed in Figure 1 with the experimental data (calculations can be found in the Supporting Information). The shear-thinning behavior observed is consistent with the presence of intermolecular interactions between molecules which are disrupted at high shear rate. A parallel can be drawn to polymers in which shear-thinning is typically the result of disruption of entanglements between polymer chains (in this case, angular frequency scans have revealed that the aggregates are too small to be entangled, see below).[17] To further support this hypothesis, the samples of compounds **5** and **9e** were found to start crystallizing after the second consecutive scan which eventually led to crystallization of the whole sample. Intriguingly, compound **9a** showed no sign of crystallization even after six consecutive scans.[18] Shearing thus seems to impact the molecular organization in a way similar to heating, by disrupting the supramolecular aggregates which would cause molecular mobility to increase. This ultimately leads to reorganization of the molecules to the more stable crystalline state, which may be slower in compound **9a** due to stronger interactions between molecules and lower conformational mobility. However, these observations deserve more thorough investigation and will be further probed in future studies.

Angular frequency scans in the oscillatory mode were then performed on the same compounds at T_g + 35 °C at a constant shear strain of 0.1%[19] to determine their time-dependent shear behavior, and the results are reported in Figure 2. In all three cases, complex viscosity was found to be constant as a function of angular frequency (Figure 2a), and storage (G') and loss moduli (G'') both increased exponentially with frequency (Figure 2b). Furthermore, no crossover point between G' and G'' or maximal values for G' and G'' was observed in the frequency range scanned, which for polymers is indicative of low molecular weight, narrow mass distribution, and little entanglement between chains,[17] hinting that the hydrogen-bonded aggregates formed are of relatively small size, confirming previous observations made with FTIR.[11]

The rheological properties of compounds **1**−**9** as a function of temperature were then studied by performing a cooling−heating scan at a rate of 2 °C/min between roughly T_g − 20 °C and T_g + 80 °C in oscillatory mode with an amplitude of 0.1% and an angular frequency of 10 s^{-1}. Only the complex viscosity curves of the heating scans can be found in Figure 3 as there is a good agreement between the heating and cooling scans (the cooling curves are shown in Figure S1, Supporting Information). Of all compounds studied, only chloromethyl derivative **2** was not reported because of thermal degradation upon prolonged heating.[20] For all compounds studied, viscosity ranged from 10^6 to 10^7 Pa·s at temperatures lower than T_g, except for compounds **5** and **7** which were slightly lower, then decreased sharply to reach a plateau with a viscosity of 1 Pa·s at approximately T_g + 50 °C. These values are significantly lower than for both inorganic glasses and polymers, which show viscosities on the order of 10^{12} Pa·s at T_g[7] but are situated in the lower range of viscosities observed for molecular glasses at T_g (10^7−10^{12} Pa·s).[7,9] Arguably, these lower viscosity values are due to "repeating units" being held together by weaker noncovalent bonds. For most compounds, the T_g values observed by rheology were slightly higher than the ones recorded by differential scanning calorimetry (DSC), which is attributed to the shear rate used. One particular feature which could be observed in most of the studied molecular glasses is a sharp rise in viscosity in the vicinity of T_g. Interestingly, this peak is absent in compounds **5**, **7**, and **8**, perhaps due to the presence of a headgroup containing a hydrogen-bonding acceptor which has been shown to be capable of participating in self-assembly, providing those compounds with two possible hydrogen bonding motifs between molecules (as can be seen in the crystal structure of compound **7**).[10] The fact that this feature is present in most compounds studied herein, with the exception of specific cases with a common structural element, suggests that it is not an artifact due to the apparatus. Nonetheless, the origins of this phenomenon are still unknown and will be the object of future studies. Other than the presence or absence of this peak, the evolution of viscosity as a function of temperature relative to T_g is closely related for all compounds of the series, so though structure of the headgroup has a tremendous impact on T_g, it has little incidence on viscosity. The molecular causes of glass transition thus seem to be similar for all compounds of the series,

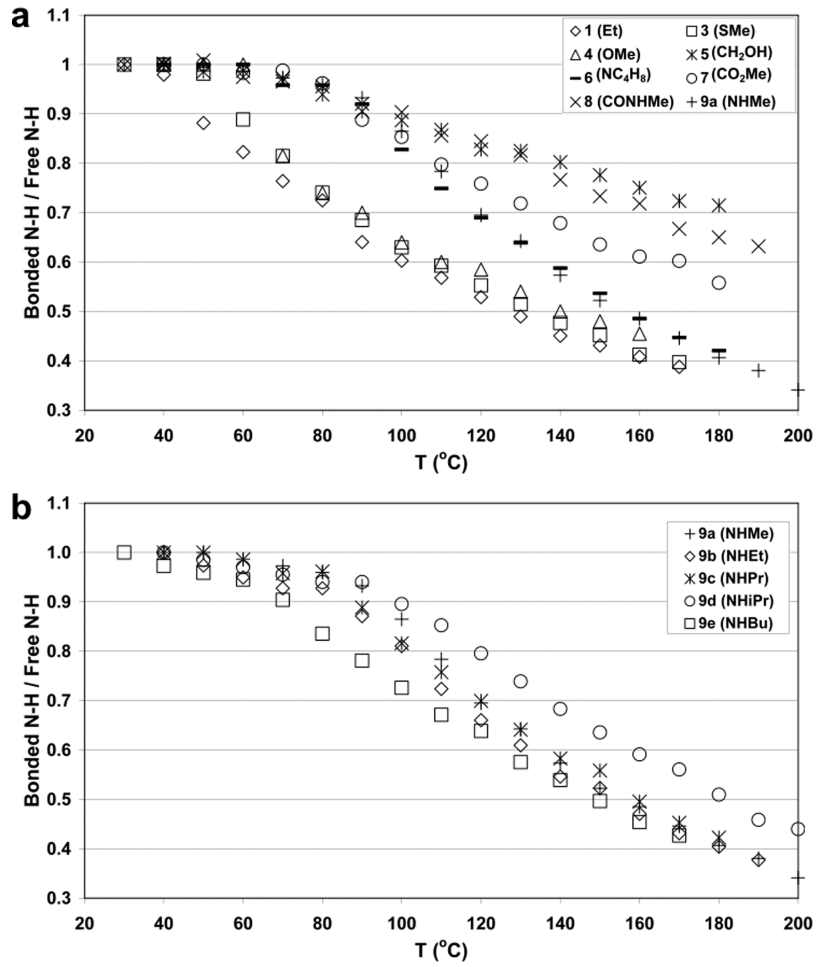

Figure 6. Normalized ratios of bonded N−H vs free N−H signals in the FTIR spectra of triazines (a) **1**−**9a** and (b) **9a**−**9e** as a function of temperature. Only the heating scans are shown for clarity. The previously published results for compound **4** are shown for reference, and the data for compound **9f** were omitted because of crystallization.

the structure of the headgroup only determining at what temperature glass transition is initiated.

Storage moduli (G') for heating scans are shown in Figure 4, and loss moduli (G'') are reported in Figure 5 (cooling scans in Figures S2−S3, Supporting Information). For all compounds studied, G' and G'' show similar trends with a sharp decrease after the compounds undergo glass transition, which is a behavior typical of amorphous materials. The G' values typically decrease from 10^7-10^8 Pa below T_g to roughly 10 Pa at T_g + 30 °C, and structural relaxation peaks can also be observed for most compounds and reflect the results of the viscosity curves. G'' values were found to reach a maximum in the range of 10^7-10^8 Pa at T_g as expected and decrease to 1 Pa in the vicinity of T_g + 80 °C. For compounds **5**, **6**, and **7**, a hump can be noticed in the G' slope in the T_g + 10 to T_g + 20 °C range. However, there does not seem to be any relationship between this hump and any particular feature of the headgroup, and no crystallization was observed in that temperature range.

Variable-Temperature FTIR Spectroscopy. FTIR spectroscopy of an amorphous sample of compound **4** at various temperatures had previously revealed that, as the material underwent glass transition, hydrogen bonds started breaking at an increased rate.[11] Since the rheology results tend to parallel those findings, the FTIR experiments were repeated on compounds **1**−**9** (except for compound **2**) to validate the existence of a relationship between hydrogen bonding and viscosity. The spectra were recorded on a cooling−heating cycle at a heating/cooling rate of 2 °C/min, typically in the same temperature range as the rheology experiments (the spectra can be found in Figure S4−S15, Supporting Information). Under these conditions, only compound **9f** could not give satisfactory results as it quickly crystallized. As with compound **4**, the relative intensity for the free and hydrogen-bonded NH stretching bands at 3410−3380 and 3300−3273 cm^{-1}, respectively, were determined. The normalized ratios of bonded vs free NH groups for the heating scans of compounds **1**−**9** are reported in Figure 6.[21] There is a good agreement between the cooling (Figure S16, Supporting Information) and heating scans, though bonded/free ratios tend to reach lower values at elevated temperatures in the heating scans. The values previously published for compound **4** were included for reference. It should be noted that because of overlaps between bands (including O−H and amide N−H stretching bands for compounds **5** and **8**) and because the determination of the absorption coefficients for the bonded N−H and free N−H signals depends on an extrapolation that is very sensitive to experimental error (the slight differences observed between the heating and cooling scans result in rather large discrepancies in calculated absorption coefficients), the hydrogen bonding indices are not absolute molar fractions and therefore can not be used directly to compare two different compounds. Their evolution with temperature, for any given compounds, is nevertheless reliable and highly reproducible. From Figure 6, it can be seen that, as for compound **4**, the derivatives studied herein show a sharp change of slope in the hydrogen bonding index in the vicinity of T_g. However, a comparison of hydrogen bonding and viscosity as a function of temperature for com-

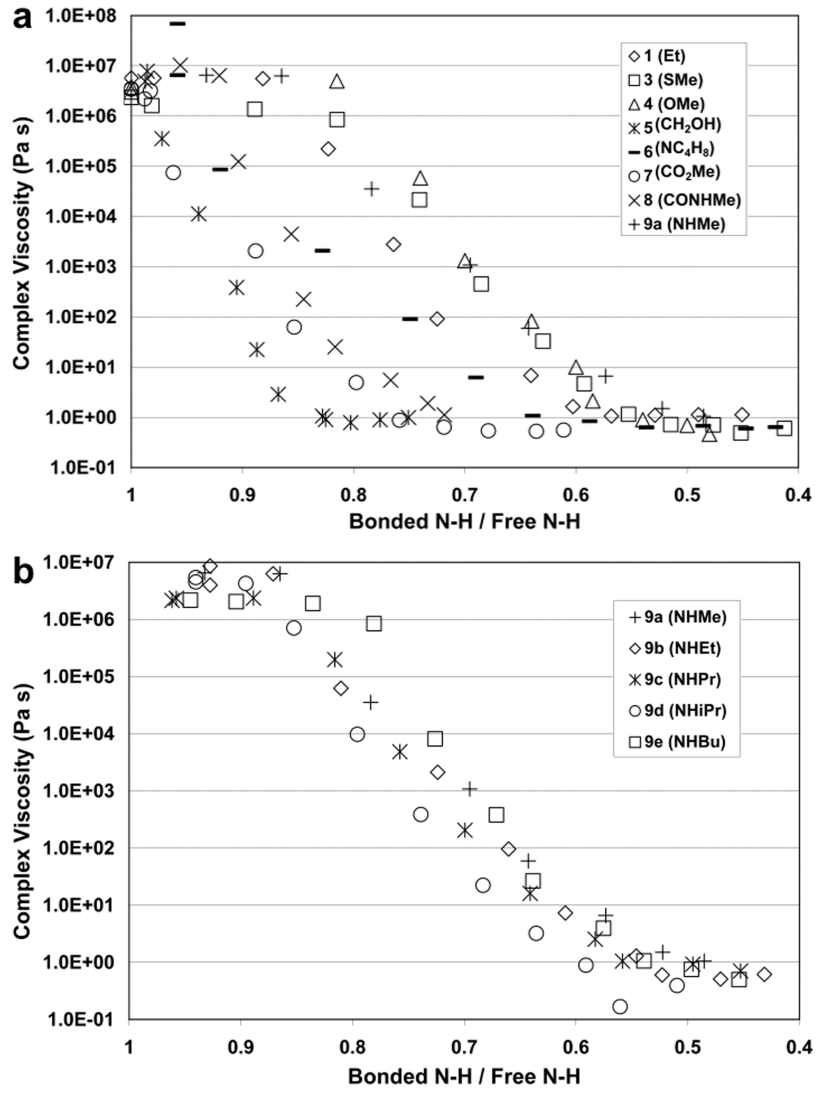

Figure 7. Complex viscosity as a function of hydrogen bonding index for molecular glasses (a) **1**−**9a** and (b) **9a**−**9e**. Only the heating scans are shown for clarity, and the data for compound **9f** were omitted because of crystallization.

pounds **1**−**9**, illustrated in Figure 7 as a graph of viscosity as a function of hydrogen bonding, reveals that (1) viscosity decreases much more sharply than hydrogen bonding and (2) the hydrogen bonding index continues to decrease even after viscosity has reached its minimum. While there exists a relationship between the two phenomena as evidenced by both being triggered concurrently at a similar temperature, this correlation is nonetheless not direct. This can be rationalized by the fact that the initial disruption in hydrogen bonding observed at T_g causes an important reduction in the size of aggregates, thereby resulting in a large increase in aggregate mobility accompanied by a sharp decrease in viscosity. At elevated temperatures, the material eventually reaches a state heavily populated with monomers where further disruption of remaining aggregates has little impact on molecular mobility.

Variable-Concentration NMR Spectroscopy. So far, a relationship was established between hydrogen bonding in this family of molecular glasses and both the physical events accompanying glass transition and their rheological properties. However, there are no significant differences between compounds of this series in their behavior other than the temperature at which glass transition is triggered. Therefore, it would be intuitive to think that the differences in T_g observed for closely similar compounds are a consequence of varying hydrogen bonding strengths between molecules of different compounds. Since hydrogen bonding strength could not be quantified with FTIR, the effect of hydrogen bonding strength on T_g for a series of similar compounds with various headgroups was studied by measuring the association constants (K_a) of selected compounds using variable-concentration ^{1}H NMR.[22] While the association of the studied molecular glasses in solution does not necessarily reflect their behavior at the molecular level in the solid state due to dilution and presence of solvent, measuring their association constants in solution can nonetheless help comparing hydrogen bonding strength for the different compounds.

^{1}H NMR spectra were recorded in $CDCl_3$ at various concentrations ranging from 1 mM to saturation for compounds **1**−**9a**. The N−H peaks from all compounds exhibited a dependency to concentration, indicative of association by hydrogen bonding (tables and curves of chemical shift as a function of concentration are available in the Supporting Information). The association constants have been calculated for all compounds using the WinEQNMR2[14] software and are shown in Table 1. All compounds studied have shown association constants in the range 0.7−2.1 M^{-1}, which are consistent with the association constant measured for 2,4-diamino-6-dodecyl-1,3,5-triazine (2.2 M^{-1}).[23] The relationship between K_a and T_g tends toward linearity, as shown in Figure 8. However, this relationship is

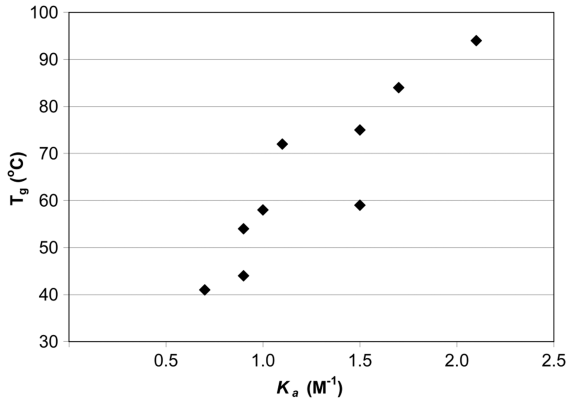

Figure 8. Graph of T_g as a function of K_a for molecular glasses **1**−**9a**. K_a values were calculated from variable-concentation ^{1}H NMR data.

TABLE 1: Association Constants (K_a) of Compounds 1−9a in $CDCl_3$ Solution[a]

compound	R	T_g (°C)	K (M^{-1})
1	−Et	41	0.7
2	$-CH_2Cl$	44	0.9
3	−SMe	54	0.9
4	−OMe	58	1.0
5	$-CH_2OH$	59	1.5
6	−pyrrolidinyl	72	1.1
7	$-CO_2Me$	75	1.5
8	−CONHMe	84	1.7
9a	−NHMe	94	1.5 (MeNH) 2.1 (ArNH)

[a] T_g are included for reference.

not perfectly linear ($R = 0.82$), as additional features of the headgroup such as alkyl chain length, polarity, and rotation barrier, for example, might also have an effect on T_g.

Slight variations in headgroup structure have been shown to translate into large differences observed in both T_g and association constant. One structural feature which can rationalize this phenomenon for some compounds of the series is the presence of strong electron-donating substituents which are conjugated to the triazine ring and thus increase its electron density, in turn making the ring nitrogen atoms more nucleophilic and stronger hydrogen bond acceptors. This effect can be exemplified with compounds **1**, **3/4**, and **6/9a**−**f** in which the headgroup shows increasing conjugation with the triazine ring.[24] Additional hydrogen bonding sites on the headgroup can also increase the association constant by providing a higher number of possible association motifs. For example, compounds **9a**−**f** possess an additional N−H group which can engage in hydrogen bonding, while the headgroups of compounds **5**, **7**, and **8** contain hydroxy or carbonyl oxygen atoms which can provide alternative hydrogen bond acceptors.

Conclusion

These studies have demonstrated that the rheological properties of bis(mexylamino)triazine-based glasses are consistent with those of other molecular glasses and support our model in which individual molecules self-assemble through hydrogen bonding to form small aggregates which interact poorly with each other, giving rise to glass formation. Disruption of these hydrogen bonds results in rupture of the aggregates and causes a decrease in viscosity, G' and G'', as a consequence of increased molecular mobility. The hydrogen bonding index as a function of temperature was monitored using FTIR spectroscopy, and a comparison of viscosity and hydrogen bonding has revealed that while both decrease abruptly once T_g is reached their decay profiles do not overlap. Instead, once hydrogen bonding falls below a certain threshold, viscosity decreases exponentially then eventually reaches a plateau where further hydrogen bond disruption has no effect. The impact of hydrogen bonding on viscosity thus seems to be related to aggregate size which is a key parameter in detemining molecular mobility in the bulk material. A correlation between T_g and association constant was uncovered, which further suggests that disruption of hydrogen bonding between molecules is the major molecular mechanism leading to glass transition in this family of compounds. However, this relationship displays significant deviation from linearity, thereby hinting that other structural factors also play a role in determining glass transition. These observations have contributed to consolidate our model to explain the behavior of this family of molecular glasses and have helped identify areas which deserve further investigation such as, in particular: (1) the effect of shearing and other mechanical stresses on supramolecular structure, (2) the role played by other structural features on T_g and rheological properties, and (3) the relationship between kinetics of crystallization and molecular structure.

Acknowledgment. We are grateful to the Royal Military College of Canada and NSERC for funding. We would also like to thank Dr. Philip Bates for access to the rheometer.

Supporting Information Available: Additional rheology scans of compounds **1**−**9**, variable-temperature FTIR spectra of compounds **1**−**9**, plots and tables of ^{1}H NMR chemical shifts of N−H groups as a function of concentration for compounds **1**−**9**, along with data calculated by WinEQNMR2. This material is available free of charge via the Internet at http://pubs.acs.org.

References and Notes

(1) For example, see: (a) Pearson, R. G. *Plastics Rubber* **1976**, *1*, 21–22. (b) Pearson, G. H.; Garfield, L. J. *Polym. Eng. Sci.* **1978**, *18*, 583–589. (c) Rojo, E.; Muñoz, M. E.; Santamaria, A.; Peña, B. *Macromol. Rapid Commun.* **2004**, *25*, 1314–1318.

(2) (a) Ozawa, T. *Polymer* **1971**, *12*, 150–158. (b) Kotek, J.; Raab, M.; Baldrian, J.; Grellmann, W. *J. Appl. Polym. Sci.* **2002**, *85*, 1174–1184.

(3) (a) Kwack, T.-H.; Han, C.-D. *J. Appl. Polym. Sci.* **1983**, *28*, 3419–3433. (b) Oyanagi, Y.; Kubota, K. *J. Polym. Eng.* **1986**, *7*, 47–75. (c) Chivers, R. A.; Moore, D. P. *Polymer* **1994**, *35*, 110–116.

(4) For example, see: (a) Shirota, Y. *J. Mater. Chem.* **2000**, *10*, 1–25. (b) Strohriegl, P.; Grazulevicius, J. V. *Adv. Mater.* **2002**, *14*, 1439–1452. (c) Shirota, Y. *J. Mater. Chem.* **2005**, *15*, 75–93. (d) Grazulevicius, J. V. *Polym. Adv. Technol.* **2006**, *17*, 694–696. (e) Shirota, Y.; Kageyama, H. *Chem. Rev.* **2007**, *107*, 953–1010.

(5) For example, see: (a) Angell, C. A. *Science* **1995**, *267*, 1924–1935. (b) Ediger, M. D.; Angell, C. A.; Nagel, S. R. *J. Phys. Chem.* **1996**, *100*, 13200–13212. (c) Hancock, B. C.; Zografi, G. *J. Pharm. Sci.* **1997**, *86*, 1–12. (d) Yu, L. *Adv. Drug Delivery Rev.* **2001**, *48*, 27–42.

(6) (a) Hancock, B. C.; Shalaev, E. Y.; Shamblin, S. L. *J. Pharm. Pharmacol.* **2002**, *54*, 1151–1152.

(7) For example, see: (a) Angell, C. A.; Ngai, K. L.; McKenna, G. B.; McMillan, P. F.; Martin, S. W. *J. Appl. Phys.* **2000**, *88*, 3113–3157. (b) Gutzow, I.; Grigorova, Ts.; Todorova, S. *J. Non-Cryst. Solids* **2002**, *304*, 4–18. (c) Roland, C. M. *Soft Matter* **2008**, *4*, 2316–2322.

(8) Naito, K. *Chem. Mater.* **1994**, *6*, 2343–2350.

(9) (a) De Rosa, M. E.; Adams, W. W.; Bunning, T. J.; Shi, H.; Chen, S. H. *Macromolecules* **1996**, *29*, 5650–5657. (b) Boils, D.; Perron, M.-È.; Monchamp, F.; Duval, H.; Maris, T.; Wuest, J. D. *Macromolecules* **2004**, *37*, 7351–7357.

(10) Lebel, O.; Maris, T.; Perron, M.-È.; Demers, E.; Wuest, J. D. *J. Am. Chem. Soc.* **2006**, *128*, 10372–10373.

(11) Wang, R.; Pellerin, C.; Lebel, O. *J. Mater. Chem.* **2009**, *19*, 2747–2753.

(12) Wuest, J. D.; Lebel, O. *Tetrahedron* **2009**, *65*, 7393–7402.

(13) Since we could not quantify the absolute molar fraction of N−H groups participating in hydrogen bonding in the samples, the concept of hydrogen bonding index is used herein in a qualitative fashion to describe differences in hydrogen bonding as a function of temperature.

(14) Hynes, M. J. *J. Chem. Soc., Dalton Trans.* **1993**, 311−312. Software available on request at: michael.j.hynes@nuigalway.ie.

(15) This temperature was chosen because viscosity is low enough that the apparatus does not reach shear stress limit at high shear rate.

(16) Carreau, P. J.; De Kee, D. *Can. J. Chem. Eng.* **1979**, *57*, 3–15.

(17) Mezger, T. G. *The Rheology-Handbook*; Zorll, U., Ed.; Vincentz: Hannover, 2002.

(18) The high resistance of compound **9a** to crystallization under thermal conditions was already reported. See ref 11.

(19) Frequency scans were performed at various amplitudes, but the results did not vary significantly.

(20) No degradation was observed in the same temperature range by DSC, possibly because the DSC measurement was taken under nitrogen atmosphere. Chlorinated polymers such as PVC are known to degrade upon heating: Fuchsman, C. H. *SPE J.* **1959**, *15*, 787–790.

(21) For ease of comparison, bonded N−H vs free N−H ratios (which were calculated by comparing the heights of the respective bands) were normalized to a value of 1 for the measure taken at the lowest temperature for each data set. Thus, for every sample, the bonded N−H vs free N−H ratio for every temperature was divided by the ratio taken at the lowest temperature.

(22) Fielding, L. *Tetrahedron* **2000**, *56*, 6151–6170.

(23) Beijer, F. H.; Sijbesma, R. P.; Vekemans, J. A. J. M.; Meijer, E. W.; Kooijman, H.; Spek, A. L. *J. Org. Chem.* **1996**, *61*, 6371–6380.

(24) While the CH_2 group of compound **1** rotates freely, triazine amines (such as the headgroups of compounds **6** and **9**) are known to be hybridized sp^2 (see refs 10 and 11) and display rotational barriers on the order of 18 kcal/mol: Hyengoyan, A. P.; Mamyan, S. S.; Gomktsyan, T. A.; Hambardzumyan, E. N.; Vorskanyan, A. S.; Eliazyan, K. A.; Pivazyan, V. A.; Dovlatyan, V. V. *Chem. Heterocycl. Compd.* **2005**, *41*, 1059–1061.

JP905268A